

AD 613296



TECHNICAL REPORT

Lexington Laboratories, Inc.

84 SHERMAN STREET
CAMBRIDGE, MASS. 02140
Area Code 617 • 864-5020

EVALUATION OF VAPOR DEPOSITION GROWTH OF
OXIDE SINGLE CRYSTALS FROM METAL HALIDES

Prepared by:

Philip S. Schaffer - Lexington Laboratories, Inc.

Contract No. Nonr-4574(00)
ARPA Order No. 306

Quarterly Technical Summary Report No. 2
1 August 1964 - 31 October 1964

Physical Sciences Division
Office of Naval Research
Washington, D. C. 20360

ARCHIVE COPY

COPY	2	OF	3
HARD COPY	\$.		
MICROFICHE	\$.		

TABLE OF CONTENTS

	Description	Page No.
1.0	SUMMARY	2
2.0	OBJECTIVES	3
3.0	EXPERIMENTAL PROCEDURE	4
4.0	RESULTS AND DISCUSSIONS	6
4.1	Growth Parameters	6
4.2	Kinetic Consideration	12
4.3	Dislocation Density	17
5.0	FUTURE WORK	20
6.0	BIBLIOGRAPHY	21

TABLE OF FIGURES

Figure No.	Description	Page
1	Bulk Crystal Growth Rate vs. Reactant Vapor Velocity and Total Pressure (at constant reactant gas partial pressure ratios)	9
2	Bulk Crystal Growth Rate vs. Substrate Temperature (at constant total pressure, reactant gas pressures)	10
3	Bulk Crystal Growth Rate vs. p_{H_2} / p_{CO_2} (at constant p_T , T , p_{AlCl_3} , p_{CO_2} , p_{CO})	10

TABLE OF FIGURES

Figure No.	Description	Page
4	Single Crystal Alpha-Alumina Fibers on 60° Orientation Alpha-Alumina Substrate. 2.1 x.	11
5	Alpha-Alumina Vapor Grown Crystal and Substrate. 2x.	13
6	Bulk Crystal Growth Rate vs. 1/T	15
7	Etch Pits on {1120} Plane of Alpha-Alumina Substrate (bottom) and Chromium-Doped Alpha-Alumina Vapor Overgrowth (top). 200x.	18
8	Etch Pits on {0001} Plane of Vapor Grown Alpha-Alumina c-Axis Platelet. 186x.	19

This is the second in the series of quarterly technical summary reports on "Evaluation of Vapor Deposition Growth of Oxide Single Crystals from Metal Halides" for the Department of the Navy (ONR) under Contract No. Nonr-4574 (00). This report is intended only for the internal management uses of Lexington Laboratories, Inc., and the Department of the Navy (ONR).

1.0 SUMMARY

Preliminary investigations to determine significant vapor growth parameters have been completed. Growth rate, substrate orientation and temperature, reactant vapor velocity, total pressure and partial pressures of the reactant gases have been shown to influence the kinetics of crystal growth from the vapor phase. Optimum growth conditions based on these parameters will be established by future work.

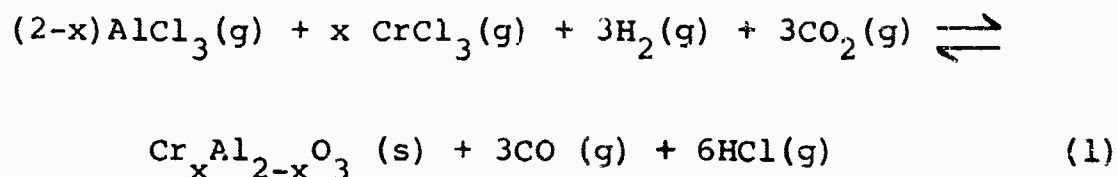
A two-inch diameter, molybdenum-element, muffle furnace has been completed, which will enable growth of oriented ruby and sapphire crystals at least one inch in diameter. It is presently being utilized in the growth parameter investigations.

An experimental activation energy of 3.25 ev was determined for the overall growth process. A mechanism other than gaseous diffusion appears to be dominant for this system. Laminar flow, in the growth zone, is indicated by a calculated Reynolds number of 13.5.

Polishing and etching by chemical techniques have been used to reveal the dislocation density of basal $\{0001\}$ and prism $\{11\bar{2}0\}$ planes on sapphire and ruby crystals grown by the vapor technique and flame fusion process. Vapor grown crystals exhibited a density reduction of one to three orders of magnitude over the flame fusion substrates. It has been observed that dislocation densities decreased with increasing thickness of vapor growth.

2.0 OBJECTIVES

This program is designed to determine and evaluate the significant parameters for the vapor phase growth of chromium-doped, alpha-alumina (ruby) and alpha-alumina (sapphire). A detailed investigation will be made to determine the variables which influence the formation kinetics of the reaction system represented by the following equation when $x \geq 0$.



Experimental apparatus will be designed, constructed and utilized for the growth of crystals at least one inch in diameter. Spectrochemical and optical analyses will be made to determine the concentration and degree of chromium homogeneity of the crystals. The relation between dislocation density (etch-pit technique) and the purity of starting materials will be investigated.

3.0 EXPERIMENTAL PROCEDURE

A two-inch diameter, molybdenum-element, muffle furnace has been constructed and utilized in growth parameter investigations. This furnace will facilitate the growth of oriented ruby and sapphire crystals at least one inch in diameter. Modifications in the vapor train and furnace assemblies have been made to attain higher purity in vapor grown crystals.

Investigations have been conducted to relate the growth rate (growth velocity) of alpha-alumina with the process parameters of vapor phase growth. These parameters include substrate temperature, total pressure, crystal orientation, reactant vapor velocity and partial pressures of the reactant gases. A set of standard conditions was established permitting only one or a minimum number of growth variables during each growth experiment. Optimum conditions can be established by correlating the growth rates to the degree of crystalline perfection.

Dislocation density, which is directly related to the degree of internal strain present in a crystal, is used as a measure of crystalline perfection. Chemical polishing and etching techniques^{1,2} were utilized to reveal dislocation structures for {0001} and {11 $\bar{2}$ 0} planes in sapphire and ruby crystals. The basal surface was chemically polished in 85% orthophosphoric acid (H_3PO_4) at 425°C for 150 seconds. Etching in potassium bisulfate ($KHSO_4$) at 675°C for 15-20 seconds developed triangular pits on the {0001} planes. The prism planes {11 $\bar{2}$ 0} were polished with potassium aluminum fluoride (K_3AlF_6) at 1000°C for 45

seconds. Polygonal etch pits were developed on these planes by etching in KHSO_4 at 675°C for 135 seconds. Samples were preheated prior to immersion in the reagents to minimize thermal shock. Platinum crucibles were used to contain the heated etchants. Temperature measurement was achieved with platinum - platinum 10% rhodium thermocouples.

4.0 RESULTS AND DISCUSSION

4.1 Growth Parameters

At a temperature of 1750°C, a total pressure of 9.0 torr and constant partial pressure ratios of the reactant gases, growth velocity was measured on 60° alpha-alumina, rod substrates. A range of velocities was obtained by varying the flow rates of the reactant gases and maintaining a constant total pressure by throttling the vacuum pumping system.

Figure 1 shows the rate of bulk crystal growth as a function of average reactant vapor velocity and total pressure. For laminar flow, the shape of the velocity-distribution curve is parabolic; therefore, the velocity at the center of the tube where bulk crystal growth occurs is twice the average velocity. The growth rate changed from negligible growth at a velocity of 300 cm/sec to a maximum at approximately 1170 cm/sec and decreased with increasing velocity. The low growth rate at lower velocities is attributed to deposition on the furnace walls prior to the reactant gas stream reaching the substrate. At very high velocities, the short gas residence time suppressed kinetic processes which cause growth to proceed by material transport across the substrate-vapor boundary.

A vertical line, G, was drawn at a growth rate of 100 $\text{mg/cm}^2 \cdot \text{hr.}$ which represents the maximum observed rate. This rate was established as $\Delta G = 0$. Higher growth rates as related to velocity and/or total pressure would be represented as $\Delta G > 0$ while lower growth rates would be represented as $\Delta G < 0$.

In Fig. 1, the growth rate was measured a function of total pressure at a temperature of 1750°C and constant partial pressures. The total pressure was varied by throttling the vacuum pumping system. At low pressures, (high velocities) very short gas residence times resulted in low growth rates. Maximum growth occurred at a total pressure of approximately 9.0 torr (velocity, 1170 cm/sec). At higher pressures (lower velocities) which increase the residence time, deposition on the furnace walls may increase. Lower growth rates may also be attributed to homogeneous nucleation. Also, at higher pressures, the supersaturation increases to favor powder formation. These homogeneously nucleated powders are submicron particles of alumina (0.05 microns diameter in 1 micron agglomerates).

In Fig. 2, the growth rate is shown as a function of substrate temperature at constant total and partial pressures. At 1550°C, little bulk crystal growth occurred, although fiber formation was abundant. Growth rate was maximum at 1800°C. From free energy determinations discussed previously³, ΔF_R° becomes more negative with increasing temperature indicating that the overall reaction (1) becomes more favorable. From kinetic considerations, the rate of reaction is greater with increasing temperature; therefore, above 1800°C the lower growth may be attributed to two factors. The first is that the rate of evaporation of Al_2O_3 molecules from the substrate surface is greater than the rate of condensation. Secondly, because of the higher temperature at essentially uniform reactant gas velocities, depletion of the reactant vapor stream may occur by increased deposition on the furnace walls.

The growth rates shown in Fig. 1 were measured on crystals grown at a constant substrate temperature of 1750°C. Since the growth rate is maximum at 1800°C, rate measurements made at this temperature should result in $\Delta G > 0$, indicating more favorable conditions for bulk crystal growth. Growth rates below those obtained at 1750°C should result in $\Delta G < 0$.

Figure 3 shows the bulk crystal growth rate as a function of the ratio of the hydrogen partial pressure to the carbon dioxide partial pressure. Total pressure, substrate temperature and partial pressures of aluminum chloride, carbon dioxide and carbon monoxide were held constant. Partial pressure of hydrogen and changes in velocity were the only variables. The growth rate increased continuously with higher hydrogen partial pressure up to a ratio of 7:1 where the gas velocity was 1540 cm/sec. It was shown in Fig. 1 that increasing the velocity above 1170 cm/sec (under described conditions) resulted in a decrease in growth rate. The partial pressure ratio may be more of a contributing factor to reaction completion than to the velocity.

From Fig. 3 it appears that the p_{H_2}/p_{CO_2} limit may have been approached. The increased growth rate achieved by increasing the hydrogen partial pressure may be attributed to excess hydrogen reaction with chlorine forming hydrogen chloride, further driving the overall reaction to completion.

Figure 4 shows single crystal sapphire fibers grown on a 60° sapphire substrate. These fibers grew with preferred orientation up to 0.008 inch diameter and 0.5

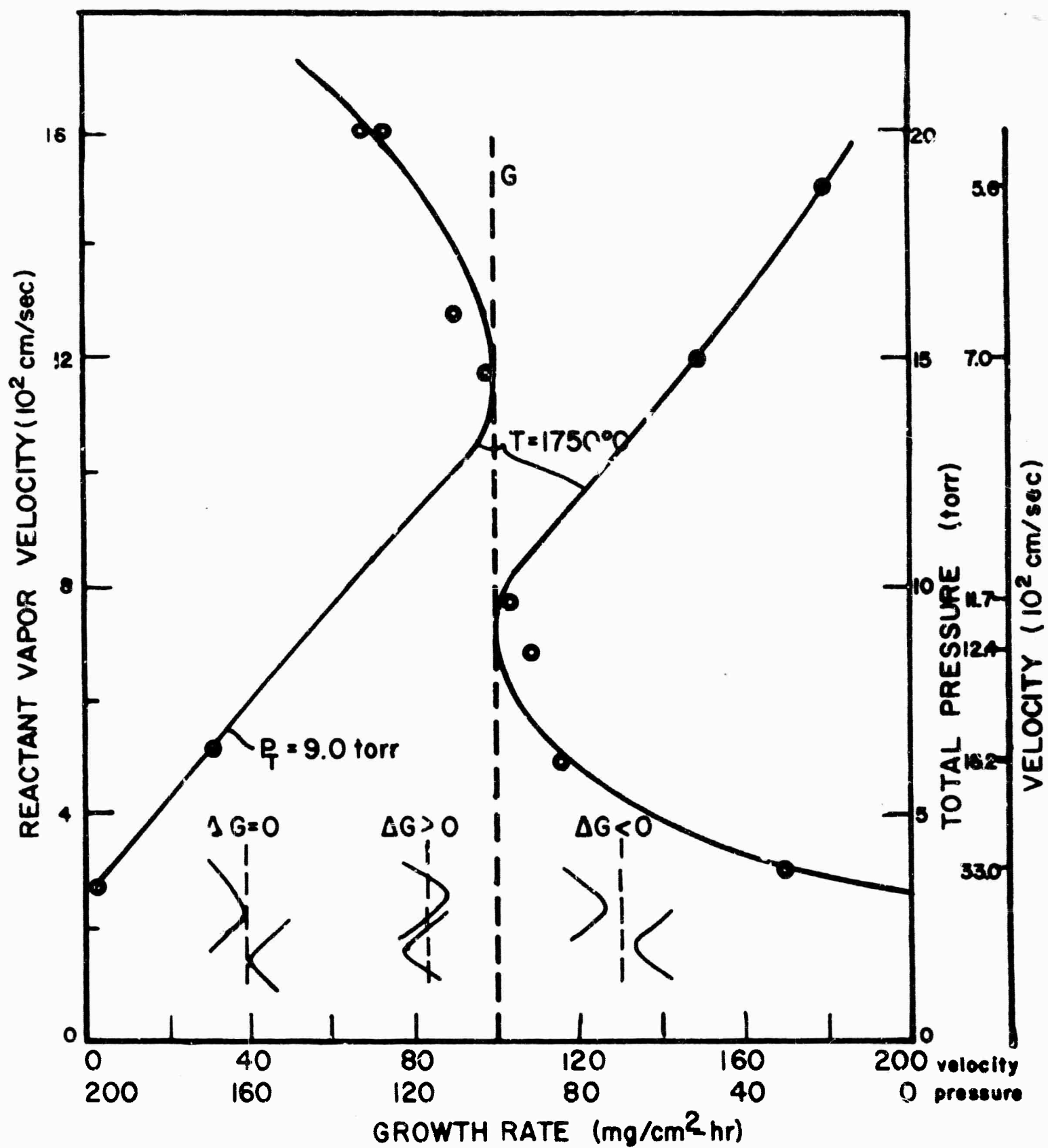


Figure 1: Bulk Crystal Growth Rate vs. Reactant Vapor Velocity and Total Pressure (at constant reactant gas partial pressure ratios)

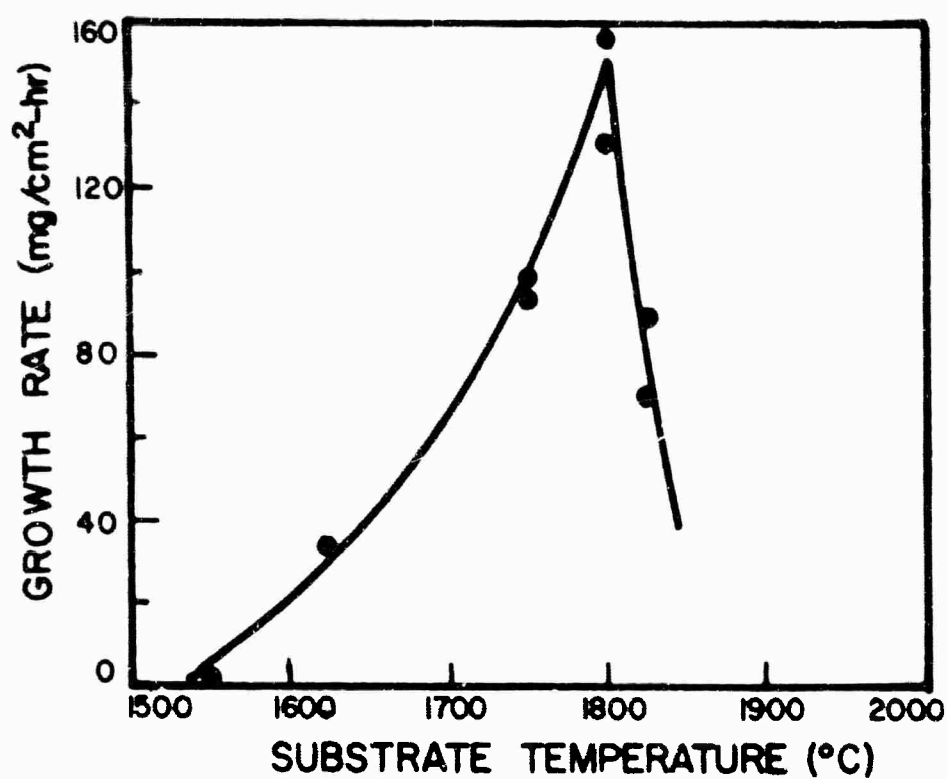


Figure 2: Bulk Crystal Growth Rate vs. Substrate Temperature (at constant total pressure, reactant gas pressures)

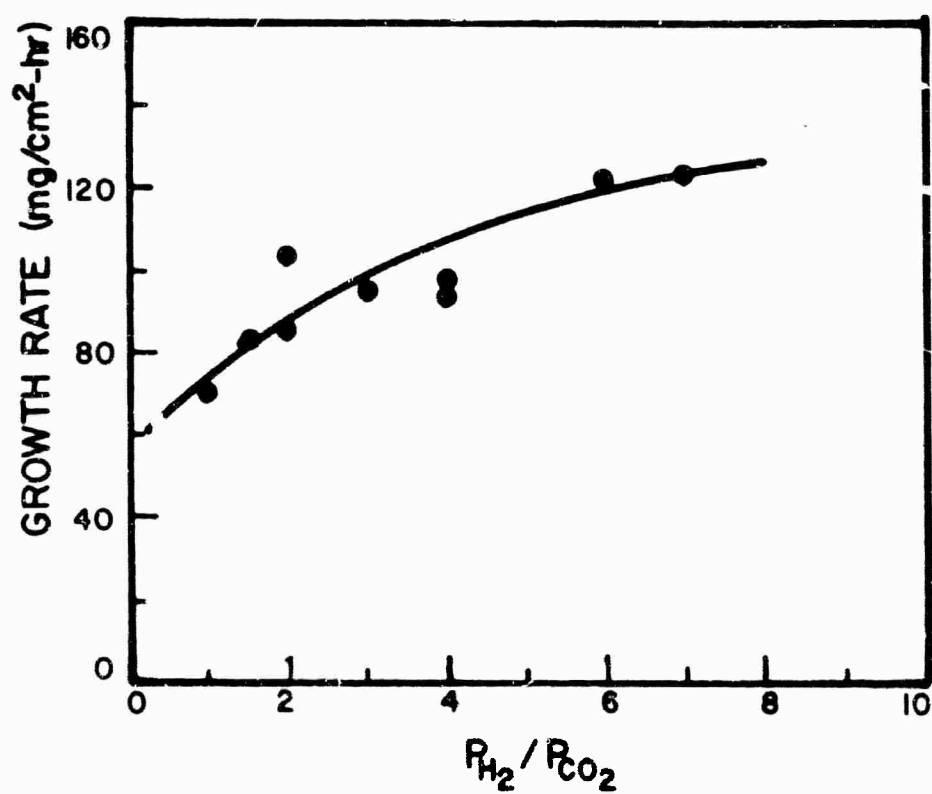


Figure 3 - Bulk Crystal Growth Rate vs. P_{H_2}/P_{CO_2} (at constant P_T , T , P_{AlCl_3} , P_{CO_2} , P_{CO})

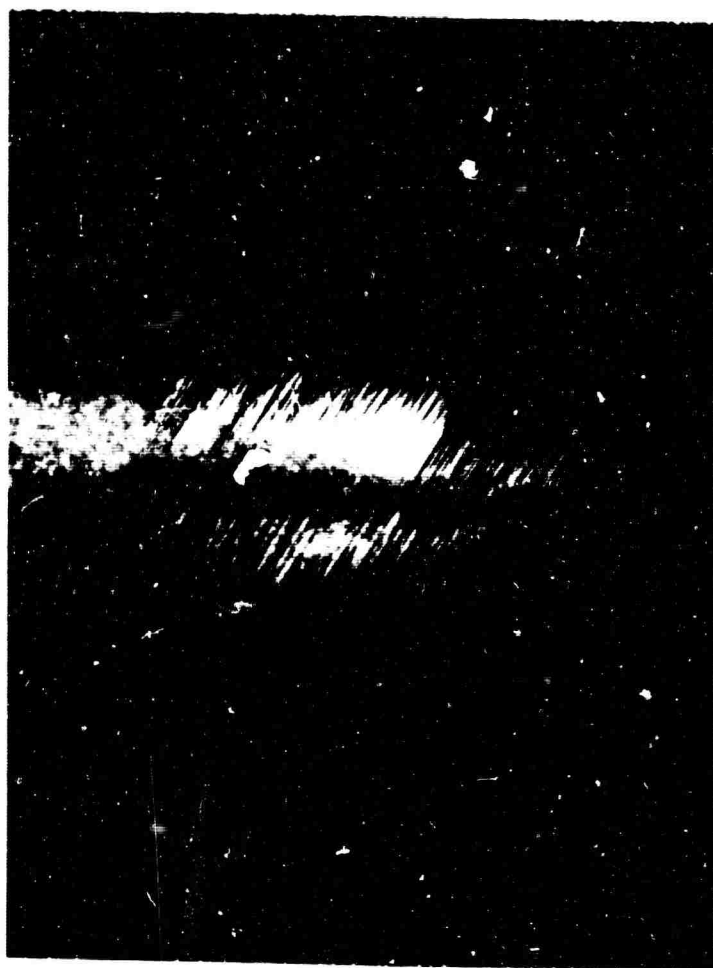


Figure 4: Single Crystal Alpha-Alumina Fibers on 60° Orientation Alpha-Alumina Substrate. 2.1x.

inch long in two hours. Lowering the temperature changed the degree of supersaturation to the region where fiber growth was favorable and bulk crystal growth was negligible. This effect shows that the degree of completion of the reaction was decreased by decreasing temperature.

Growth rate as a function of crystallographic orientation is being measured. Figure 5 shows a spherical substrate and a crystal produced by three hours of growth. Preliminary investigations indicate the existence of three distinct sets of crystallographic planes in the vapor grown crystal. These are the basal plane $\{0001\}$ (in the plane of the photograph), prism planes $\{11\bar{2}0\}$ (perpendicular to the plane of the photograph) and a set of planes, either $\{22\bar{4}3\}$ or $\{11\bar{2}2\}$, approximately 50° from the c-axis, increasing in growth velocity, respectively. Exact determination of the latter plane by optical goniometry methods was difficult due to the vicinal faces developed in the planes by the vapor growth technique.

4.2 Kinetic Considerations

Bulk crystal growth rate plotted as an inverse logarithmic function of the substrate temperature yielded a straight line, Fig. 6. This suggests that the vapor growth process, condensation of a supersaturated vapor, is a first order reaction and can be represented by the Arrhenius relationship:

$$G = G_0 \exp (-Q/RT) \quad (2)$$



Figure 5 - Alpha-Alumina Vapor Grown Crystal and Substrate.
2x.

where G = bulk crystal growth rate ($\text{mg}/\text{cm}^2\text{-hr}$)

G_0 = growth constant

Q = experimental activation energy of the growth process

R = molar gas constant (1.99 cal/mole)

T = absolute temperature ($^{\circ}\text{K}$)

The experimental activation energy, Q , is 3.25 eV ($74,930 \text{ cal/mole}$). In order for crystal growth to occur by gaseous diffusion, the growth rate must vary as $T^{3/2}$ (Ref. 4). Since the data do not obey this relationship, it is suggested that another mechanism may be involved in the condensation process.

The kinetics of the overall process for the transfer of material during condensation from a supersaturated vapor involve (a) transport of reactant vapors to the substrate-vapor boundary layer, (b) reaction at this boundary layer, that is deposition on the substrate and (c) transport of gaseous products away from this layer.

At the elevated substrate temperatures used in the growth of alpha-alumina, it seems likely that the rate controlling process is the diffusion of material across the substrate-vapor boundary layer. Although the degree of supersaturation will determine the morphological species formed, under conditions where bulk crystal growth is favorable and homogeneous nucleation is minimized, increasing the velocity and subsequently the Reynolds number to an optimum value, the growth rate will increase as the rate at which the reactant gases reach the substrate and diffusion of material across the substrate is increased.

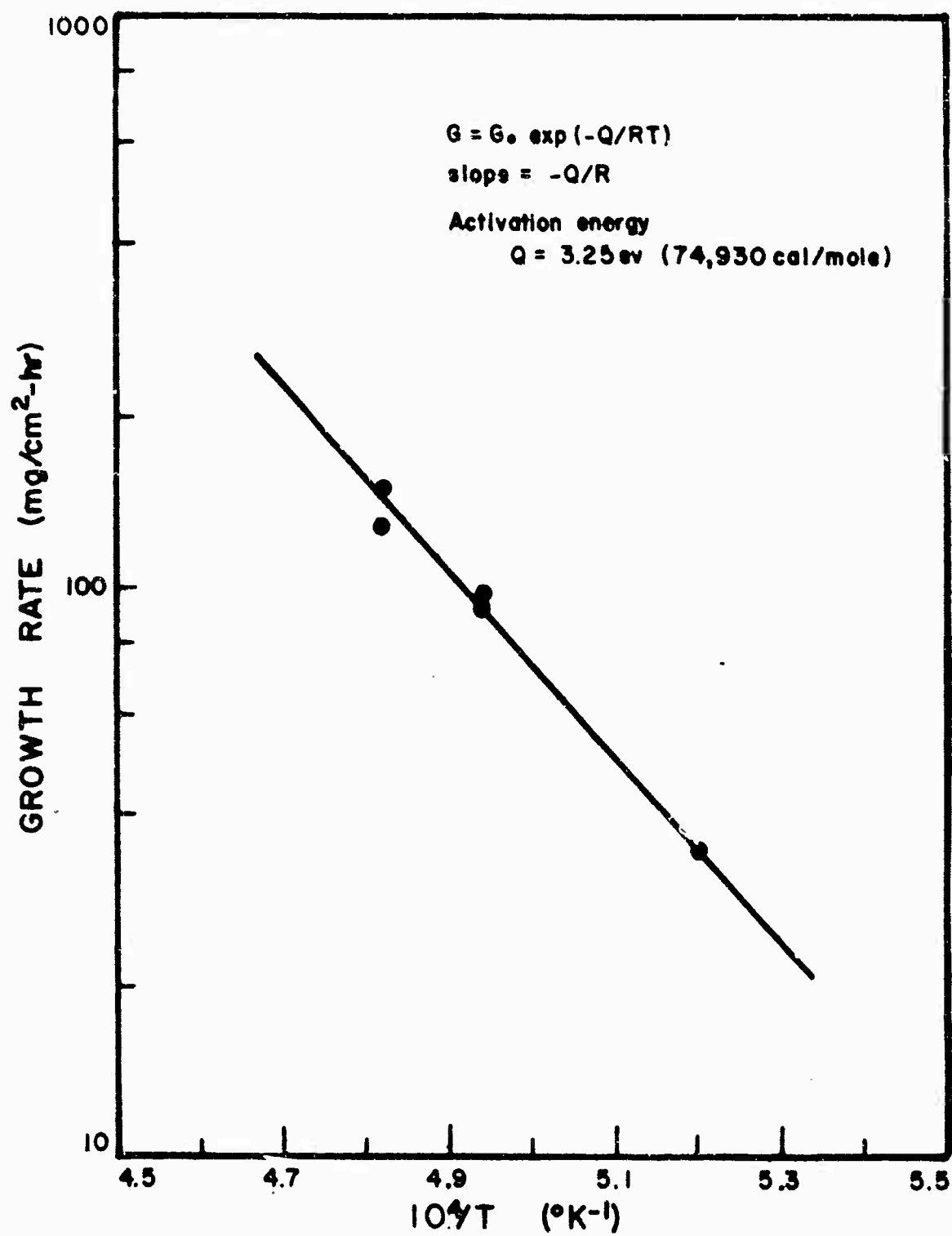


Figure 6 - Bulk Crystal Growth Rate vs. $1/T$

To determine the type of flow existing in the growth zone, the Reynolds number, N_{re} , was calculated:

$$N_{re} = \frac{dv}{\mu} \quad (3)$$

where d = diameter of growth zone

v = velocity of reactant vapor stream

μ = kinematic viscosity = $\frac{\nu(\text{viscosity})}{\rho(\text{density})}$ = stokes

Under the standard growth conditions, the velocity in the growth zone was calculated as follows:

$$v_{STP} = \frac{(1,907 \text{ cm}^3/\text{min})}{(60 \text{ sec/min}) (15.8 \text{ cm}^2)} = 2.01 \text{ cm/sec}$$

$$v \text{ (at } 1750^\circ\text{C, } 9.0 \text{ torr)} = (v_{STP}) (T_0/K/293) (760/P_{\text{torr}}) =$$

$$1,173 \text{ cm/sec}$$

$$\mu = \frac{\nu}{\rho} = \frac{5.46 \times 10^{-4} \text{ poise}}{1.46 \times 10^{-6} \text{ gm/cm}^3} = 3.90 \times 10^2 \text{ stoke}$$

$$N_{re} = \frac{dv}{\mu} = \frac{(4.5 \text{ cm}) (1.173 \times 10^3 \text{ cm/sec})}{(3.90 \times 10^2 \text{ gm-cm}^3/\text{sec-gm-cm})} = 13.5$$

For this value of N_{re} , based upon the average velocity, laminar flow exists, i.e., molecular vapor flow occurs parallel to the longitudinal axis of the furnace chamber without an appreciable radial component. At high N_{re}

values, approximately 2×10^3 , the flow is turbulent due to the existence of vortexes or eddy currents in the growth zone. Increasing the Reynolds number from 13.5 would increase the transport of material across the substrate-vapor boundary.

4.3 Dislocation Density

Figure 7 shows the prism plane $\{11\bar{2}0\}$ of an alpha-alumina substrate with vapor overgrowth of ruby in the upper portion. The sub-boundaries extend into the overgrowth from the substrate. The dislocation density of the substrate is 4.9×10^6 pits/cm² compared to 6.2×10^5 per cm² for the ruby overgrowth. Ruby specimens⁵ (0.30 wt % Cr₂O₃) showed an increase of 25% in dislocation density compared to sapphire, both grown by the Verneuil process. However, there is a reduction of 87.3% from the substrate to the ruby overgrowth in Fig. 7. The $\{0001\}$ face of a vapor-grown c-axis platelet with a dislocation density of 3.8×10^3 per cm² is shown in Fig. 8. Dislocation density tends to decrease with increasing thickness of vapor overgrowth. Vapor grown crystals exhibited a density reduction of one to three orders of magnitude over their flame fusion substrates.



Figure 7: Etch Pits on {1120} Plane of Alpha-Alumina Substrate (bottom) and Chromium-Doped Alpha-Alumina Vapor Overgrowth (top). 200x.

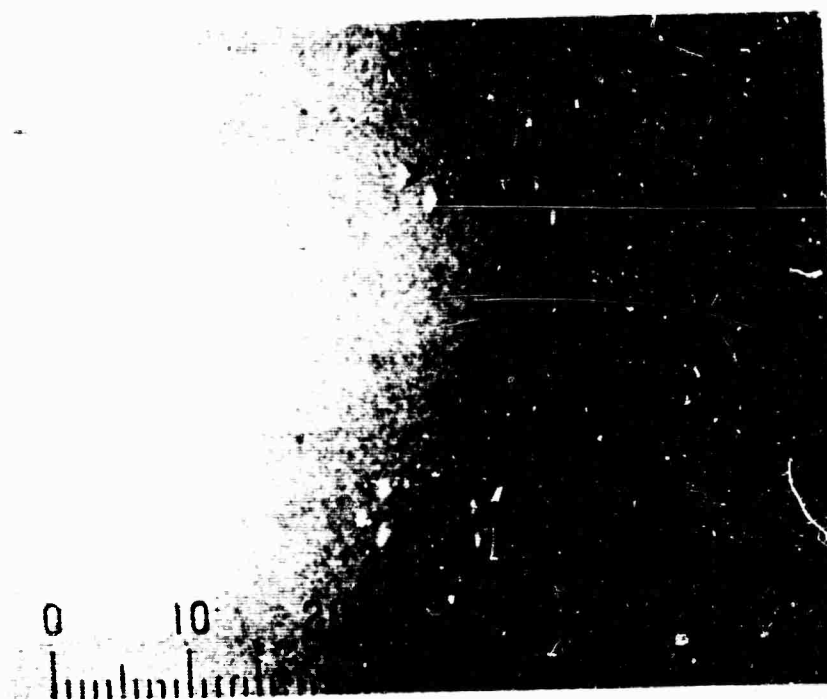


Figure 8: Etch Pits on $\{0001\}$ Plane of Vapor Grown Alpha-Alumina c-Axis Platelet. 186x.

5.0 FUTURE WORK

The investigation of growth velocity as a function of substrate orientation and partial pressure of $\text{AlCl}_3(\text{g})$ will be continued. A correlation will be made of growth velocity as a function of crystalline perfection, as indicated by dislocation density. Optimum growth parameters of substrate temperature, total pressure, orientation, reactant vapor velocity and partial pressures of the reactant gases will then be established for the vapor growth technique.

Using optimum growth parameters, the study of vapor phase growth of chromium-doped alpha-alumina will be continued. Single crystals at least one inch in diameter will be grown; spectrochemical and optical analyses will be made to determine the chromium concentration and degree of homogeneity.

The effect of high purity starting materials on dislocation density and crystal purity will be determined.

6.0 BIBLIOGRAPHY

1. Scheuplain, R. and Gibbs, P., "Surface Structure in Corundum:1, Etching of Dislocations", J. Am. Cer. Soc., 43, (9), 458-471, (1960)
2. Alford, W. J. and Stephens, D. L., "Chemical Polishing and Etching Techniques for Al_2O_3 Single Crystals", J. Am. Cer. Soc., 46, (4), 193-194 (1963).
3. Schaffer, P. S. and Campbell, W. B., "Evaluation of Vapor Deposition Growth of Oxide Single Crystals from Metal Halides", Quarterly Technical Summary Report No. 1, Nonr-4574(00), July, 1964.
4. Bird, R. B., Steward, W. E. and Lightfoot, E. N., Transport Phenomena, Wiley and Sons, Inc., 510, 1960.
5. Stephens, D. L., and Alford, W. J., "Dislocation Structures in Single Crystal Al_2O_3 ", J. Am. Cer. Soc., 47, (2), 81-86, (1964).